Available online at www.sciencedirect.com

ScienceDirect

Ceramics International 40 (2014) 1235–1239

CERAMICS INTERNATIONAL

www.elsevier.com/locate/ceramint

Short communication

Effects of growth temperature on nitrogen incorporation into InGaPN epilayer and its optical properties

Kang Min Kim[a,b], Shigehiko Hasegawa[b], Hajime Asahi[b], Jeong Ho Ryu[c,*]

[a]National Institute of Advanced Industrial Science and Technology, 1-1-1 Umezono, Tsukuba 305-8568, Japan
[b]The Institute of Scientific and Industrial Research, Osaka University, 8-1 Mihogaoka, Ibaraki, Osaka 567-0047, Japan
[c]Department of Materials Science and Engineering, Korea National University of Transportation, Chungbuk 380-702, Republic of Korea

Received 7 May 2013; received in revised form 3 June 2013; accepted 3 June 2013
Available online 17 June 2013

Abstract

The effect of growth temperature on the nitrogen concentration and optical properties of the InGaP(N) epilayer was investigated. The nitrogen concentration of InGaPN is dependent on the growth temperature (450–490 °C), whereas the indium concentration is independent of the growth temperature. Nitrogen concentration decreased the photoluminescence (PL) intensity and increased the full width at half maximum of the PL peak. Raman analysis revealed that the preferred atomic configuration of InGaPN consisted of Ga–N and In–P bonds, which induced higher local strains during growth. The degradation of PL efficiency was related to this bonding configuration. Nitrogen concentration reduced the coupling constant of electron–phonon interaction, thus, reducing the temperature dependence of the PL peak shift. The reduced PL quenching around room temperature was attributed to the decrease of band discontinuity at the InGaPN/GaAs heterointerface due to the increase in N concentration.

Keywords: A. Films; C. Optical properties; D. Nitrides; InGaPN

1. Introduction

Dilute nitrides have received considerable attention due to their unusual physical properties and potential optoelectronic applications [1,2]. Especially, the InGaPN quaternary alloys can be lattice-matched to GaAs [3], GaP [4], and Si [5] substrates by adjusting their indium and nitrogen concentrations. Therefore, this material system has been proposed for various applications in electronic and optoelectronic devices, such as heterojunction bipolar transistors [6], laser diodes [7], and tandem solar cells [8]. However, like InGaAsN, InGaPN still suffers from low photoluminescence efficiency due to the large difference in the atomic radius between the group III sources and N, which dramatically degrades the crystallinity of InGaPN. Hence, as-grown samples of dilute nitrides contain a high number of defects [9–12] such as N interstials, As_{Ga} antisites and Ga vacancies, which act as non-radiative centers that induce the degradation of optical efficiency. In the case of the InGaAsN system, it was reported that the defect problem may be alleviated by low temperature growth [13]. However, only a few reports have been published on the effect of growth temperature on the optical properties and N concentration of InGaPN. Moreover, high N concentrations may cause strong PL quenching, broaden the PL line-width, increase non-radiative recombination, and thus lower the material gain and increase the transparency carrier density to a level similar to the case of InGaAsN QWs [14,15]. Hence, a detailed understanding of the PL quenching mechanisms of InGaPN alloys is essential to gain insight into the mechanisms contributing to the change in PL efficiency of InGaPN compound semiconductors.

In this study, we report the influence of growth temperature on the N concentration and optical properties of InGaPN epilayers also the possible growth mechanisms that may degrade these effects will be discussed.

2. Experiments

The samples in this study were grown on semi-insulating GaAs (100) substrates by gas-source molecular-beam epitaxy. Elemental In (7N) and Ga (7N) were used as the group III sources, and thermally cracked AsH_3, PH_3 and ion-removed,

*Corresponding author. Tel.: +82 438415384; fax: +82 438415380.
E-mail addresses: jimihen@hanyang.ac.kr, jhryu@ut.ac.kr (J.H. Ryu).

0272-8842/$ - see front matter © 2013 Elsevier Ltd and Techna Group S.r.l. All rights reserved.
http://dx.doi.org/10.1016/j.ceramint.2013.06.009

electron cyclotron resonance (ECR) plasma-assisted N_2 [16] were used as the group V sources. Initially, a GaAs buffer layer of 200 nm was grown at 560 °C, followed by the growth of the InGaPN eplilayer. The substrate temperature during the growth of the epilayer was varied from 450–490 °C. Constant beam fluxes of the group III and group V sources were used for the entire range of growth temperatures. The thicknesses of the $In_xGa_{1-x}P_{1-y}(N_y)$ epilayers were 500 nm. Growth was monitored by in situ reflection high-energy electron diffraction (RHEED). In and N concentrations were calibrated from X-ray diffraction (XRD) measurements by first determining the In concentration from the InGaP thin film and then determining the N concentration from InGaPN, assuming that the In concentration remained unchanged.

Raman spectra were measured at room temperature using Reinshaw in Via Raman microprobe with backscattering from the (100) growth surface under 532 nm laser excitation. PL spectra were measured by using a 488-nm line of an Ar-ion laser as the excitation light source and an InGaAs photodiode as the detector. The excitation laser light was focused onto the sample through a lens. PL measurements were carried out at temperatures from 10 K–300 K by mounting the samples in a closed cycle cryostat.

3. Results and discussion

Fig. 1 shows the 10 K PL spectra for the InGaP(N) samples grown under basically identical conditions, but at different growth temperatures of 450, 475, and 490 °C. With increasing growth temperature, the PL spectra show a blueshift, even when the nitrogen beam flux was kept the same. To investigate the effect of growth temperature on indium incorporation in the InGaP grown at different growth temperatures, XRD measurements were carried out. In the temperature range of 450–490 °C, the In composition does not depend on the temperature (inset of Fig. 1). This result is in good agreement with previous reports [17,18]. However, the nitrogen concentrations of the InGaPN samples were dependent on growth temperature. The N content in InGaPN decreased with increasing growth temperature, as shown in the inset of Fig. 1. Therefore, this blueshift in the PL spectra with increasing growth temperature was related to the reduction of the N content in InGaPN. Compared with the PL spectra of the InGaP sample, those of the InGaPN samples showed an asymmetric line shape with a sharp, high-energy cut off and an exponential, low-energy tail. Also, the increase in the full width at half maximum (FWHM) of the PL peak and the reduction of the PL intensity are observed. This degradation of PL is related to the introduction of nitrogen into InGaP, similar to the case of InGaAsN. During the epitaxial growth of InGaAsN, it was found that the favorable bond configuration consisted of Ga–N and In–As bonds due to their large cohesive bond energies [19]. However, this bonding configuration induces high local strains owing to the different bonding lengths, unlike the In–N and Ga–As bonds [19]. Hence, composition modulation and surface roughness increased. In the present case as well, a similar situation is considered: the

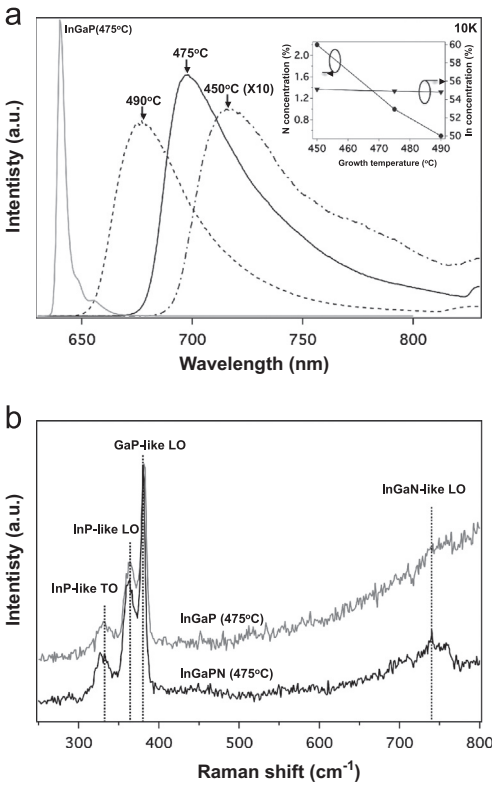

Fig. 1. (a) PL spectra of InGaP(N) samples grown at different growth temperatures measured at 10 K. The inset shows the indium concentration of InGaP (inverse triangles) and the nitrogen concentration of InGaPN (circles) as a function of growth temperature. (b) Raman spectra for InGaP and InGaPN samples grown at 475 °C.

Ga–N and In–P bond configurations, which induces higher strains due to the difference in the bonding lengths of InP, GaP, InN, and GaN of 2.54, 2.36, 2.15, and 1.94 Å, respectively [20,21], which are preferable in an InGaPN material system.

In order to verify our expectation concerning the bond configuration, we carried out Raman measurements. Fig. 1(b) shows the Raman spectra of InGaP and InGaPN samples grown at 475 °C. The Raman spectrum of InGaP consists of GaP-like longitudinal optic (LO) phonon mode at 381 cm^{-1}, InP-like LO phonon mode at 364 cm^{-1}, and InP-like transverse optic (TO) phonon mode at 329 cm^{-1} [22,23]. In the case of the InGaPN sample, a broad peak located around 735 cm^{-1} (between 630 and 775 cm^{-1}) is observed, as well as the InGaP peaks. Lin et al. [24] reported that the Raman peak of $In_{0.54}Ga_{0.46}P_{1-y}N_y$ ($y=0.005$–0.02) around 730 cm^{-1} corresponds to the InGaN- like LO phonon mode. The A_1 (LO) phonon mode of the binary compounds GaN and InN are located at 734 cm^{-1} and 586 cm^{-1}, respectively [25]. This broad peak is located closer to the A_1 (LO) phonon mode of GaN. It can be inferred that the Ga–N bonds contribute more to the InGaN-like LO phonon mode than the In–N bonds. Therefore, the favorable bond configuration under our growth condition consists of Ga–N and In–P bonds in this material system.

The temperature dependence of the PL peak energies is shown in Fig. 2 for the InGaP sample and InGaPN samples grown at different growth temperatures. For the InGaPN sample grown at T_g=450 °C with N=2.2%, PL could not be detected above 175 K, which indicated the presence of a high concentration of non-radiative centers. In the case of the InGaP sample, the peak energy red-shifts to a lower energy with increasing temperature, in good agreement with the regular temperature change. In contrast, the temperature dependence of the N-containing samples from 10 K to 150 K shows an inverted S-shape behavior, and the PL peak energy red-shifts above 175 K due to the shrinkage of the temperature-dependent bandgap energy. These phenomena indicate that the localized exciton energy states were preferentially occupied in the low temperature region and that carriers escaped from the localized states to the free energy states with increasing temperature. The solid lines represent the results of fitting using the expression for the temperature dependence of the bandgap with consideration of the electron–phonon interaction, [26,27]

$$E(T) = E_{g0} + \beta\coth(\hbar\omega_{\Gamma\gamma}/2kT) \quad (1)$$

where $\hbar\omega_{\Gamma\gamma}$ is the phonon energy of an interaction mode, β is the coupling constant of the electron–phonon interaction, k is Boltzmann's constant and E_{g0} is the genuine bandgap.

Using this expression, our experimental results were well fitted in the high temperature range (above 175 K). The fitting parameters are given in Table 1. From the Raman measurement, (as shown in Fig. 1(b)), the InP-like TO phonon mode is located at 40.7 meV. This frequency is close to the value of $\hbar\omega_{\Gamma\gamma}$ in Table 1. This finding implies that the bandgap shrinkage of InGaP systems with temperature is caused by the inter-band mixing assisted by the InP-like TO phonon at zero point.

Comparing the second term of Eq. (1), the β values for the samples, it is found that the InGaPN sample grown at 475 °C has the lowest β value due to the higher N incorporation. The temperature-insensitive bandgap in the InGaPN material system is induced by the low β value [27]. Hence, this indicates that the thermal stability of the PL peak energy above 175 K was improved by the N incorporation.

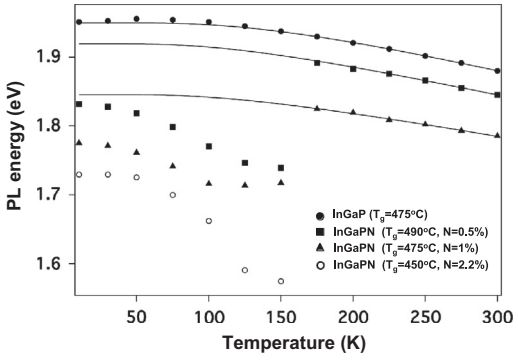

Fig. 2. Temperature dependence of the PL peak energy in the temperature range from 10 K to 300 K for the InGaP(N) samples grown at different growth temperatures. Solid lines are the curves fitted with Eq. (1).

The temperature dependence of the integrated PL intensity for the InGaPN samples grown at different temperatures was investigated in Fig. 3. According to the classical theory of thermal quenching, temperature-dependent PL intensity can be described by the expression [28]

$$I(T) = \frac{I_0}{1 + A\exp(-E_A/kT)} \quad (2)$$

where I_0 is the initial intensity, $I(T)$ is the intensity at a given temperature T, k is Boltzmann's constant, E_A is the activation energy for thermal quenching, and A is a constant determined by the ratio of radiative lifetime to non-radiative lifetime. Fig. 3 plots Ln[(I_0/I)−1] vs 1/(kT). The slopes of Fig. 3 correspond to different activation energies.

Table 1
Summary of fitting parameters with Eq. (1) from InGaP(N) samples.

Growth temperature (T_g) (°C)	Nitrogen content (%)	E_{g0} (eV)	$\hbar\omega_{\Gamma\gamma}$ (meV)	β (eV)	Sample type
450	2.2				InGaPN
475	1.0	1.91	31.5	0.07	InGaPN
490	0.5	2.00	31.8	0.09	InGaPN
475	0.0	2.07	38.7	0.12	InGaP

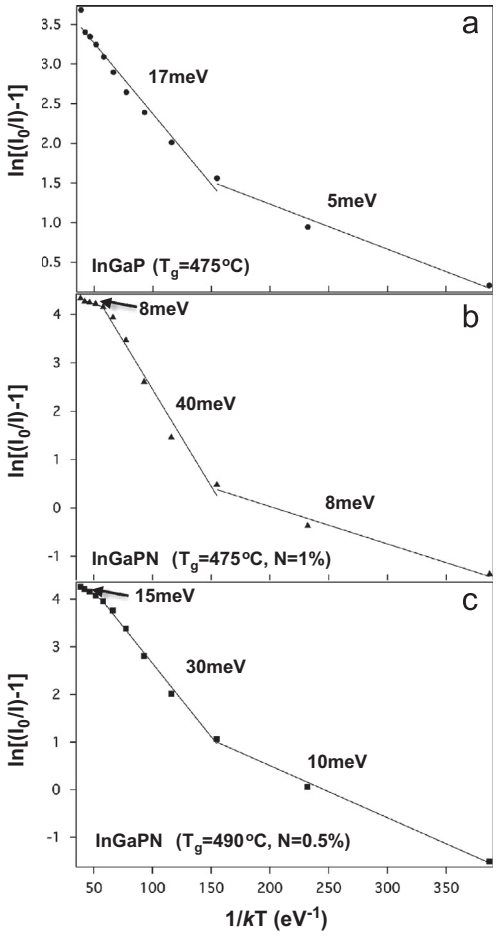

Fig. 3. Temperature dependence of the integrated PL intensity for the InGaP (N) samples grown at different growth temperatures. Solid lines are the curves fitted with Eq. (2).

As the temperature increases up to 75 K, all the samples showed a small decrease in PL efficiency, with activation energy in the range of 5–10 meV. This decrease is attributed to exciton dissociation [29]. At low temperatures, the excitons dissociate into free electron–hole pairs with increasing temperature. In this case, the probability that the carriers will be trapped by defects and/or recombined nonradiatively increases. Above 75 K, the PL quenching in the InGaPN samples behaves very differently from that in the InGaP sample. In the temperature range of 75–200 K, InGaP(N) samples showed higher PL quenching with temperature due to the thermal activation of the localized excitons/carriers to free excitons/carriers. However, PL quenching at $T > 200$ K in the InGaPN samples is reduced near room temperature with decreasing activation energy from 17 to 8 meV, unlike that of the InGaP sample. The bandgap alignment at the InGaPN/GaAs heterointerface is changed by the increase in the N content from type I to type II, which results from the N-induced downshift of the conduction band (CB) states of InGaPN [7,30]. Consequently, the reduced discontinuity at the CB allows the photo-excited electrons from CB in the GaAs-side to diffuse, or become injected, into the InGaPN-side. Hence, the higher concentration of electrons in the CB helps in the suppression of PL quenching. Therefore, the activation energy near room temperature for the InGaPN samples can be related to the discontinuity in the CB between the InGaPN-side and the GaAs-side.

4. Conclusion

In summary, we investigated the effect of growth temperature on the N content and optical properties of InGaPN grown by gas-source MBE. The N concentration in InGaPN increased with decreasing growth temperature. The preferred atomic configuration in InGaPN consisted of Ga–N and In–P bonds in the growth temperature range of 450–490 °C, as inferred from Raman measurement. This bonding configuration degraded the PL efficiency. In contrast to the PL intensity, which decreased, the PL peak energy and PL quenching around room temperature varied less with temperature than those of InGaP. Thus, InGaPN based optical devices are expected to show less temperature-variation of emission wavelength and PL quenching around room temperature than InGaP based optical devices.

References

[1] M. Kondow, K. Uomi, A. Niwa, T. Kitatani, S. Watahiki, Y. Yazawa, GaInNAs: a novel material for long-wavelength-range laser diodes with excellent high-temperature performance, Japanese Journal of Applied Physics 35 (1996) 1273–1275.

[2] J.S. Harris, GaInNAs long-wavelength lasers: progress and challenges, Semiconductor Science and Technology 17 (2002) 880–891.

[3] Y.G. Hong, F.S. Juang, M.H. Kim, C.W. Tu, Growth and characterization of GaInNP grown on GaAs substrates, Journal of Crystal Growth 251 (2003) 437–442.

[4] S.M. Kim, Y. Furukawa, H. Yonezu, K. Umeno, A. Wakahara, Effect of indium on photoluminescence properties of InGaPN layers grown by solid source molecular beam epitaxy, Japanese Journal of Applied Physics 44 (2005) 8309–8313.

[5] S. Liebich, M. Zimprich, A. Beyer, C. Lange, D.J. Franzbach, S. Chatterjee, N. Hossain, S.J. Sweeney, K. Volz, B. Kunert, W. stolz, Laser operation of Ga(NAsP) lattice-matched to (001) silicon substrate, Applied Physics Letters 99 (2011) 071109-1–071109-3.

[6] Y.G. Hong, R. Andre, C.W. Tu, Gas-source molecular beam expitaxy of GaInNP/GaAs and a study of its band lineup, Journal of Vacuum Science and Technology B 19 (2001) 1413–1416.

[7] J.S. Hwang, K.I. Lin, H.C. Lin, S.H. Hsu, K.C. Chen, Y.T. Lu, Y.G. Hong, C.W. Tu, Studies of band alignment and two-dimensional electron gas in InGaPN/GaAs heterostructures, Applied Physics Letters 86 (2005) 061103-1–061103-3.

[8] M. Bosi, C. Pelosi, The potential of III–V semiconductors as terrestrial photovoltaic devices, Progress in Photovoltaics: Research and Applications 15 (2007) 51–68.

[9] S.B. Zhang, S.H. Wei, Nitrogen solubility and induced defect complexes in epitaxial GaAs:N, Physical Review Letters 86 (2001) 1789–1792.

[10] P. Carrier, S.H. Wei, S.B. Zhang, S. Kurtz, Evolution of structural properties and formation of N–N split interstitials in $GaAs_{1-x}N_x$ alloys, Physical Review B 71 (2005) 165212-1–165212-5.

[11] N.Q. Thinh, I.A. Buyanova, W.M. Chen, H.P. Xin, C.W. Tu, Formation of nonradiative defects in molecular beam epitaxial GaN_xAs_{1-x} studied by optically detected magnetic resonance, Applied Physics Letters 79 (2001) 3089–3091.

[12] K.M. Kim, W.B. Kim, D. Krishnamurthy, J.H. Ryu, S. Hasegawa, H. Asahi, Study on nitrogen-induced defects formation and annealing effects in TlInGaAsN alloy system, Journal of Crystal Growth 368 (2013) 35–38.

[13] H.Y. Liu, C.M. Tey, C.Y. Jin, S.L. Liew, P. Navaretti, M. Hopkinson, A.G. Cullis, Effects of growth temperature on the structural and optical properties of 1.6 μm GaInNAs/GaAs multiple quantum wells, Applied Physics Letters 88 (2006) 191907-1–191907-3.

[14] E.M. Pavelescu, C.S. Peng, T. Jouhti, J. Konttinen, W. Li, M. Pessa, M. Dumitrescu, S. Spanulescu, Effects of insertion of strain-mediating layers on luminescence properties of 1.3-μm GaInNAs/GaNAs/GaAs quantum-well structures, Applied Physics Letters 80 (2002) 3054–3056.

[15] B.V. Volovik, A.R. Kovsh, W. Passenberg, H. Kuenzel, N. Grote, N.A. Cherkashin, Y.G. Musikhin, N.N. Ledentsov, D. Bimberg, V.M. Ustinov, Optical and structural properties of self-organized InGaAsN/GaAs nanostructures, Semiconductor Science and Technology 16 (2001) 186–190.

[16] K. Iwata, H. Asahi, K. Asami, S. Gonda, High quality GaN Growth on (0001) sapphire by ion-removed electron cyclotron resonance molecular beam epitaxy and first observation of (2×2) and (4×4) reflection high energy electron diffraction patterns, Japanese Journal of Applied Physics 35 (1996) L289–L292.

[17] K. Ozasa, M. Yuri, H. Matsunami, Temperature dependence of InGaP, InAlP, and AlGaP growth in metalorganic molecular-beam epitaxy, Journal of Crystal Growth 102 (1990) 31–42.

[18] S.F. Yoon, K.W. Mah, H.Q. Zheng, P.H. Zhang, Effects of substrate temperature on the properties of $In_{0.48}Ga_{0.52}P$ grown by molecular-beam epitaxy using a valved phosphorus cracker cell, Journal of Crystal Growth 191 (1998) 613–620.

[19] X. Kong, A. Trampert, E. Tournie, K.H. Ploog, Decomposition in as-grown (Ga,In)(N,As) quantum wells, Applied Physics Letters 87 (2005) 171901-1–171901-3.

[20] J.L. Martins, A. Zunger, Bond lengths around isovalent impurities and in semiconductor solid solutions, Physical Review B 30 (1984) 6217–6220.

[21] T. Mattila, A. Zunger, Predicted bond length variation in wurtzite and zinc-blende InGaN and AlGaN alloys, Journal of Applied Physics 85 (1999) 160–167.

[22] T. Kato, T. Matsumoto, T. Ishida, Raman Spectral Behavior of $In_{1-x}Ga_xP$ $(0 < x < 1)$, Japanese Journal of Applied Physics 27 (1988) 983–986.

[23] A. Hassine, J. Sapriel, P. LeBerre, M.A. DiFortePoisson, F. Alexandre, M. Quillec, Superlattice effects induced by atomic ordering on $Ga_xIn_{1-x}P$ Raman modes, Physical Review B 54 (1996) 2728–2732.

[24] K.I. Lin, J.Y. Lee, T.S. Wang, S.H. Hsu, J.S. Hwang, Y.G. Hong, C.W. Tu, Effects of weak ordering of InGaPN, Applied Physics Letters 86 (2005) 211914-1–211914-3.

[25] M.R. Correia, S. Pereira, E. Pereira, J. Frandon, E. Alves, Raman study of the A_1(LO) phonon in relaxed and pseudomorphic InGaN epilayers, Applied Physics Letters 83 (2003) 4761–4763.

[26] S. Emura, H. Sumida, S. Gonda, S. Mukai, Temperature dependence of photoluminescence spectra of the pentanary alloy semiconductor $(Al_xGa_{1-x})_{1-z}In_zP_yAs_{1-y}$, Journal of Applied Physics 64 (1988) 3292–3295.

[27] K.M. Kim, S. Emura, D. Krishnamurthy, S. Hasegawa, H. Asahi, Growth and photoluminescence properties of TlInGaAsN/TlGaAsN triple quantum wells, Journal of Applied Physics 108 (2010) 053501-1–053501-6.

[28] A. Chiari, M. Colocci, F. Fermi, Y.H. Li, R. Querzoli, A. Vinattieri, W.H. Zhuang, Temperature dependence of the photoluminescence in GaAs/GaAlAs multiple quantum well structure, Physica Status Solidi B 147 (1988) 421–429.

[29] M. Hugues, B. Damilano, J.-Y. Duboz, J. Massies, Exciton dissociation and hole escape in the thermal photoluminescence quenching of (Ga,In)(N,As) quantum wells, Physical Review B 75 (2007) 115337-1–115337-5.

[30] M. Izadifard, J.P. Bergman, W.M. Chen, I.A. Buyanova, Y.G. Hong, C.W. Tu, Photoluminescence upconversion in GaInNP/GaAs heterostructures grown by gas source molecular beam epitaxy, Journal of Applied Physics 99 (2006) 073515-1–073515-5.